

1 Scientific Justification

1.1 The AGN/Galaxy Connection

The quasar/galaxy connection is threatening to make sense, at least in theory. Key evidence that AGN and galaxy evolution are linked are (1) the tight correlations locally between central black hole masses and velocity dispersions of galaxy bulges (Ferrarese & Merritt 2000; Gebhard et al. 2000; Tremaine et al. 2002) and (2) encouraging comparisons between the local number of supermassive black holes (SMBH) and the luminosity density produced by high redshift quasars (Yu & Tremaine 2002). The process hypothesized to mediate the $M_{BH} - \sigma$ connection is feedback: quasars and supernovae associated with prodigious star formation grow in the centers of galaxies until they unbind the galactic gas that feeds them (e.g., Granato et al. 2004).

1.2 Mergers

The feedback paradigm dovetails with cosmological models of hierarchical structure formation if quasar activity is induced by massive mergers (e.g., Wyithe & Loeb 2002, 2005). The discovery in hard X-rays of binary active nuclei in local objects NGC 6240 (Komossa et al. 2003), Arp 299 (Zezas, Ward, & Murray 2003) and elsewhere (Teng et al. 2005) supports the merger scenario, but only a handful of confirmed double-nucleus AGN are known.

Why are active mergers so rare? First, they may be heavily shrouded and therefore only detectable locally as ultraluminous infrared galaxies. ULIRGs have bolometric luminosities rivalling quasars, and by some (*HST I* band) estimates, as many as 40% retain double active nuclei (Cui et al. 2001). Second, mergers may also be rare simply because the lifetime of the interacting (yet unmerged, yet resolvable) phase is extremely short (Mortlock et al. 1999), and/or because most mergers took place at high redshift. Using a suite of hundreds of hydrodynamical simulations of galaxy mergers, our models (Hopkins et al. 2005a) posit that between the (mid-merger) buried and (post-merger) dead phases, the merging system is seen as a luminous optical quasar. The models successfully reproduce observed quasar lifetimes, intrinsic lifetimes, N_H distributions, and differences between optical and X-ray samples, across luminosities from $44 < \log L_{Bol} < 47$ ($-17 < M_B < -30$).

Many binocular monsters should be merging (Khochfar & Burkert 2001) near the peak of the space density of luminous quasars at $z \sim 2$ (Wolf et al. 2003; Silverman et al. 2005). The mechanics, dynamics and timescales of such mergers are of the utmost interest. To constrain the flourishing models for mergers and AGN/galaxy feedback, we propose to observe a sample of binary quasars for study of their spectral energy distributions and environments.

1.3 Binary Quasars

Sensitive, wide-area searches are required to find candidate mergers, and at high redshifts, we expect the first such samples to skim the cream: luminous, optically bright, Type 1 quasars that are spatially resolved, but in close proximity. Until recently just a handful of these binary quasars were known. Most were found in surveys for lenses but had discrepant redshifts, and/or lacked an obvious lensing galaxy. Some of the latter cases were shown by subsequent followup to be true binaries (Kochanek, Falco & Munoz 1999; Green et al. 2002, 2004), while others remain suspiciously lens-like (e.g., due to evidence for an intervening

cluster potential – Green et al. 2005). The parent sample of binary quasars was tiny, and extremely heterogeneous.

The number of known binary quasars has recently tripled. Hennawi et al. (2005; HJ05 hereafter) searched the Sloan Digital Sky Survey (SDSS) and 2QZ quasar samples using several complementary techniques to select 221 quasar pairs having proper transverse separations $R_p < 1h^{-1}$ Mpc. They thereby extended the quasar correlation function down to scales of $10 \leq R_p \leq 400$ kpc. The $10 - 30\times$ excess over the extrapolated larger-scale quasar correlation function provides strong support that dissipative interactions trigger quasar activity in rich environments. The sample selection of HJ05 is well-characterized and probes an enormous volume ($\sim 40 \text{ Gpc}^3$) to find these extremely rare binary quasar systems, which are high redshift, luminous counterparts to local AGN mergers. We aim to study a well-chosen subsample to determine (1) do the SEDs of these close binary quasars show evidence through their spectral energy distributions for merger-induced rapid SMBH growth, starbursting, or obscuration? (2) Are they in rich, poor, or typical environments?

1.4 Spectral Energy Distributions (SEDs)

We will compare our sample quasar properties to the large and growing archival sample of single quasars similarly imaged by both *Spitzer* and *Chandra*. This includes the Boötes/NOAO Deep-Wide/AGES sample¹ (e.g., Stern et al. 2005), the Extended Groth Strip (Barmby et al. 2006), SWIRE (Lonsdale et al. 2003), and the ELIAS N1/N2 First Look Survey (e.g., Lacy et al. 2005), and others. The SEDs of normal Type 1 SDSS quasars published by Richards et al. (2006) from the latter 2 surveys is shown in Figure 1 as an example of the excellent comparison samples available. We estimate expected host galaxy contribution to the SEDs starting from the scaling relationships among L_{bulge} , M_{bulge} , M_{BH} , and the quasar L_{Edd} , together with the quasar/host luminosity relationships² of Vanden Berk et al. (2006), i.e. $\log(L_{Host}) = 0.87 \log(L_{AGN}) + 2.887 - \log(L_{Bol}/L_{Edd})$. From the distribution of measured broadband SEDs and L_{Bol} for these quasars, we will calculate the probability that the merger scenario is viable, i.e., that these quasars show evidence for triggered, high L/L_{Edd} accretion. We will detect (or constrain by upper limit) the restframe K band luminosity of the host bulge. If the local $M_{BH} - \sigma$ relation is valid, we can then estimate the SMBH mass. From the quasar SED and M_{BH} , we measure the Eddington ratio, to determine whether these quasars are indeed in high mass accretion phases. Broad emission line width measurements from existing ground-based optical spectra also serve as an important check on black hole mass (e.g., Vestergaard & Peterson 2006) and L/L_{Edd} (Warner et al. 2005). These measures have been calibrated to reverberation mapping estimates, and are now useful throughout our redshift range (from $H\beta$, MgII, and CIV). In analogy to spectroscopic binary stars, wherever evidence suggests that any pair is not simply viewed in projection, binary quasars immediately allow a third *virial* mass estimate of $M = \eta \Delta v^2 R_p / G$ where $\eta \sim 1$ is a dimensionless, but model-independent constant (e.g., White et al 1983).

Even though our binary quasar sample is by selection relatively unobscured along our sightline, predicted restframe U band (observed near-IR) for mergers are strongly dependent on details of gas and dust fraction, initial orbits, disk orientations, etc. By contrast, restframe K and 2–10 keV band predictions are robust, both for the AGN and its host. Figure 2 shows

¹PJG and PB are collaborators in the Boötes project.

²Here L_{Host} and L_{AGN} are specific luminosities at 6156\AA (SDSS r band) and we have taken L_{Bol}/L_{Edd} to be unity.

the results typical of our simulations. Restframe K is sensitive to the low-mass stars which make up the bulk of the stellar mass in the bulge. Restframe 2–10 keV X-rays allow a direct, and practically unobscured³ measure of the AGN power. At the redshifts of our sample (range 0.5 – 3, with a median of 1.7), *Spitzer* IRAC (3.6–8 μm) and *Chandra* ACIS (0.5–8 keV) sensitivity are well-matched to these restframe bandpasses.

1.5 Environments

Luminous quasars should inhabit rare peaks in the density field, and thereby serve as highly biased tracers of the dark matter. The mean overdensity around bright SDSS quasars like these is confirmed to be $3\times$ that around L^* galaxies (Serber et al. 2006). Furthermore, the number density of damped Lyman alpha systems (DLAs) per unit redshift, $n(z)$, within 6000 km s^{-1} of SDSS quasars is twice that of intervening absorbers (Russell et al. 2006). These extremely rare, luminous *binary* quasars should sample the *strongest* overdensities. Do they? With IRAC imaging of adequate depth, we can easily detect an overdensity of galaxies photometrically because early-type galaxies at a given redshift have a narrow range of colors which form a cluster “red-sequence” (Gladders & Yee 2000) that allows a photometric redshift determination. The technique has been verified by Wilson et al. (2005) in the *Spitzer* First Look Survey, and by Stanford et al. (2005) in the IRAC Shallow Survey of the Boötes field, detecting galaxy clusters to redshifts of ~ 1.4 and more. Indeed, this technique - using optical and mid-IR passbands - is poised to shatter the long-standing $z \sim 1$ cluster redshift ceiling. Our *Spitzer* survey will probe the binary quasar environment at a range of redshifts, where the IRAC FoV nicely spans 2–3 Mpc. Sensitive X-ray imaging *together with* optical/IR imaging is particularly sensitive even to poor clusters and groups with high mass-to-light ratios (Barkhouse et al. 2006).

1.6 Sample and Observing Strategy

To probe the quasar/galaxy connection, the properties of triggered AGN, and their environments, we propose to observe with *Spitzer* a subsample of 14 SDSS binary quasar pairs: all those at intermediate ecliptic latitudes ($b > 30^\circ$) with quasar velocity differences $\Delta v < 1000 \text{ km s}^{-1}$ and separations $R_p < 100 \text{ kpc}$. The separation criterion selects hosts likely to be interacting on their first or second pass. The velocity criterion removes most chance projections but also allows for hosts in a variety of environments from isolated pairs to massive clusters. Some of the largest Δv pairs may be caused by chance projections plus Hubble flow, but we do not want to de-select quasar pairs moving in deep (large σ_V) cluster potential wells. Conversely, some low Δv pairs may be in massive clusters if their interaction has already slowed them down, or if their orbits are in the sky plane.

We propose to supplement the *Spitzer* observations with *Chandra* imaging of the closest ($R_p \leq 50 \text{ kpc}$ and $\Delta v < 500 \text{ km s}^{-1}$) subsample. This will allow us to test 3 key indicators of whether close binary quasars are indeed triggered and how: (1) X-ray luminosity, (2) restframe SED, and (3) X-ray spectra or hardness information. Furthermore, *Chandra* can detect virialized hot cluster gas even when no luminous galaxy overdensity exists. Now and in the foreseeable future, only *Chandra* is capable of resolving these close pairs, and separating them from extended X-ray emission (Green et al. 2002).

³These energies are absorbed only for nearly Compton-thick AGN with $N_H \sim 10^{25} \text{ cm}^{-2}$.

Our IRAC photometry, particularly in combination with our proposed NOAO 4-meter imaging in i' and z' , will provide a 6-filter color-magnitude space, allowing a sensitive search for galaxies (especially ellipticals) out to 2–3 Mpc at the quasar redshifts (Figure 1b). We will detect overdensities by comparison to known number counts and to our own parallel images, counts will be *filtered in color* to decrease noise by isolating the redshift shells of interest.

Fourteen binary quasars represents the smallest uniform subsample still large enough to provide statistical rather than anecdotal results. A summary table of sample properties is shown below. If we detect no substantial differences between the SEDs of binary and isolated quasars at these redshifts, we will have cast considerable doubt on the massive merger scenario. At the same time, we will, with doubled efficiency, have observed a unique sample of 28 luminous quasars exquisitely matched in redshift, optical properties and environment. Removing these latter variables relieves the usual nagging caveats in comparisons e.g., of M_{BH} , L/L_{Edd} , and of two persistently unexplained luminosity *anti*-correlations, the Baldwin Effect (W_{λ}^{em} ; Baldwin 1977; Green et al. 2001), and X-ray brightness (f_X/f_{UV} ; Green et al. 1995; Strateva et al. 2006).

Although our program is on the small side of Medium, we feel the dataset is of sufficient and timely interest that we *waive proprietary rights to these data once the approved sample has been observed*.

| Binary Quasar | Position (J2000) | Redshift (z_A) | Sep θ (") | Δv (km/s) | R_p (kpc) | r'_B mag | Note |
|----------------|-------------------------|--------------------|------------------|-------------------|-------------|------------|------|
| SDSSJ0856+5111 | 08:56:25.63 +51:11:37.4 | 0.543 | 21.8 | 60 | 98.2 | 19.42 | |
| SDSSJ0955+6045 | 09:55:24.37 +60:45:51.0 | 0.716 | 18.6 | 460 | 95.5 | 20.62 | |
| SDSSJ0959+5449 | 09:59:07.46 +54:49:06.7 | 1.954 | 3.9 | 200 | 23.8 | 20.43 | CXO |
| SDSSJ1116+4118 | 11:16:11.74 +41:18:21.5 | 2.991 | 13.8 | 890 | 76.8 | 19.17 | |
| SDSSJ1124+5710 | 11:24:55.24 +57:10:57.0 | 2.311 | 2.2 | −540 | 12.7 | 19.52 | |
| SDSSJ1138+6807 | 11:38:09.21 +68:07:38.8 | 0.769 | 2.6 | 840 | 13.7 | 19.76 | |
| SDSSJ1225+5644 | 12:25:45.73 +56:44:40.7 | 2.379 | 6.0 | 970 | 35.4 | 20.52 | |
| SDSSJ1303+5100 | 13:03:26.17 +51:00:47.5 | 1.684 | 3.8 | 220 | 23.0 | 20.66 | CXO |
| SDSSJ1337+6012 | 13:37:13.13 +60:12:06.7 | 1.727 | 3.1 | −610 | 18.9 | 20.04 | |
| SDSSJ1409+3919 | 14:09:53.74 +39:20:00.0 | 2.078 | 6.8 | 480 | 40.7 | 20.86 | CXO |
| SDSSJ1508+3328 | 15:08:42.21 +33:28:02.6 | 0.878 | 2.9 | 200 | 16.0 | 20.15 | CXO |
| SDSSJ1530+5304 | 15:30:38.56 +53:04:04.2 | 1.531 | 4.1 | 230 | 25.0 | 20.53 | CXO |
| SDSSJ1719+2549 | 17:19:46.66 +25:49:41.2 | 2.172 | 14.7 | −220 | 87.5 | 19.65 | |
| SDSSJ1723+5904 | 17:23:17.42 +59:04:46.8 | 1.604 | 3.7 | −830 | 22.7 | 20.46 | |

CXO: we propose for *Chandra* observations of these pairs.

2 Technical Plan: Spitzer

We will image all 14 fields in all 4 IRAC bands. To adequately characterize the quasar SEDs, detect the stellar luminosity from the hosts, and also obtain high confidence photo- z s of elliptical galaxies at these redshifts, we need $\geq 5\sigma$ detections of L^* elliptical galaxies or fainter in all the IRAC bands. We have thus estimated the flux densities of our targets by redshifting the SED of an L^* elliptical galaxy (Figure 1), and find that a 5σ depth of 22 mag AB ($1.2 \mu\text{Jy}$, 1σ) in all 4 bands works well for all fields. The $8\mu\text{m}$ band drives the exposure times, so we have estimated using the online SENS-PET the number of 100-second frames required for 5σ detections at $8\mu\text{m}$. For each source we used the appropriate background level. Most of our targets are at high ecliptic latitude and have low backgrounds ($< 7 \text{ MJy/sr}$) at $8\mu\text{m}$. For a few that had "medium" backgrounds (up to 10 MJy/sr), we have imposed some loose (months-long) time window constraints that bring all targets into the low background regime. Our required depth necessitates 67 100-sec frames.

The required number of frames ranges from 17-36, confirming that 100-second frametimes are appropriate. We implement the observations using the medium cycling dither pattern. No mapping is required, since the quasar pairs are very close ($< 20''$) and any galaxy clusters surrounding them should subtend $\lesssim 3'$ (1 Mpc) at any of these redshifts.

Target SDSS J1723+5904 has a $K = 4.3$ star $3.5'$ away. This object is in the Spitzer Continuous Viewing Zone, and for certain position angles the star will fall into the 'stray light' regions around the IRAC arrays. Since we are doing very deep observations, there is sufficient redundancy to reject any stray light 'splashes' so we have not attempted to time-constrain the AOR to eliminate these. A more serious concern is SDSSJ1225+5644 which has a $K_s = 1.34$ star $6.2'$ away. For this object we can constrain the observations to be in the second half of the visibility period. This prevents the bright star from falling in the "off source" field of view and creating residual images, or falling into the stray light regions.

Confusion will be an issue in these observations particularly in the 3.6 and $4.5 \mu\text{m}$ bands. Prior knowledge of the source positions (from optical imaging) and use of point-spread-function fitting should aid in deriving accurate fluxes. We note that the smallest separation of our binary quasars is $2.2''$, just slightly larger than the IRAC FWHM at $8\mu\text{m}$. Deriving separate SEDs for that pair will be challenging; we expect to make use of the TFIT program developed by the GOODS Legacy Program and distributed by the SSC (Grogin et al 2005). This program uses positional information from higher-resolution (eg, optical) imaging together with the IRAC PSF to derive robust SEDs from crowded-field imaging.

Data reduction for these observations is expected to be straightforward. We will use the MOPEX software to mosaic the data, and TFIT to do PSF-fitting and flux extraction. The P.I., Green, leads this collaboration of experienced multiwavelength observers and theorists. Barmby is responsible for the bulk of the *Spitzer* image analysis and photometry, which is essentially in a pipeline mode after her extensive relevant work to date. Aldcroft will analyze the *Chandra* images. Barkhouse will observe at the NOAO 4m and reduce those MOSAIC images. Hopkins will run a suite of simulations that reproduce the sample distribution in redshift, Δv , separations θ , and luminosity, which we will contrast to the observed SEDs to constrain probable gas fractions, bulge masses, and accretion rates. Green will combine the catalog datasets for analysis and comparison to extant isolated quasar samples and write the bulk of the papers.

2.1 Technical Plan: *Chandra*

We propose *Chandra* imaging of 5 binary quasars from our *Spitzer* sample with $R_p \leq 50$ kpc and $\Delta v < 500$ km s⁻¹. These are virtually certain to be interacting, and for the foreseeable future only *Chandra* is capable of resolving these close pairs and separating them from any extended X-ray (host cluster) emission (see e.g., Green et al. 2002). For the quasars, we seek to characterize the X-ray luminosity and the overall SED. X-ray spectra will constrain the continuum shape and total intrinsic line-of-sight column density.⁴ With ~ 100 counts in ACIS-S for each quasar, we can constrain the f_X/f_{opt} to 5% of the observed range for AGN. Even at $z \sim 2$ we can determine N_H to $10^{21.7}$ (90% confidence limits assuming a typical X-ray power-law photon index Γ frozen at 1.9). Taking the median broadband X-ray flux of SDSS quasars in the ChaMP (see below) means we require 20 ksec per system, for a total request of 100 ksec. While ACIS-S (chip S3) covers the entire IRAC FoV, we will also benefit from wider field data using chip S4 and ACIS-I, in faint mode. There are no bright X-ray sources within $< 20'$ of our targets.

A primary goal of our proposal is to compare the multiwavelength properties of these close binary quasars to those of isolated quasars. The perfect comparison sample is available already through the PI's leadership of the Chandra Multiwavelength Project (ChaMP): 120 SDSS quasars from DR3 (Weinstein et al. 2005), matched to *Chandra* serendipitous X-ray sources we have measured in 149 X-ray images from Cycles 1 & 2. These isolated quasars have $0.5 < z < 2.4$ and $17 < r' < 21$, very similar to our binary quasar sample. Their X-ray/optical flux ratios⁵ range from about 1 to 10 ($\log f_X/f_r = -0.36 \pm 0.41$) so there is large scatter. Furthermore, there is no strong dependence on optical magnitude (or on X-ray hardness). Given also that the binary quasars – even when optically selected – may have different SEDs and/or absorption or obscuration, it is difficult to make precise estimates of X-ray brightness based on optical magnitude. We therefore simply assume above the median broadband X-ray flux of SDSS quasars in the ChaMP: 3.2×10^{-14} erg cm⁻² s⁻¹.

Compared to red sequence methods, *X-ray cluster detection* is less affected by projection effects and less biased towards more evolved galaxy populations. Multi-wavelength cluster detection schemes help to insure a higher degree of completeness and reliability in any cluster compilation (Postman 2002). Despite the presence of quasar emission, in our proposed exposure times we know (Aldcroft & Green 2003) that we can detect extended cluster emission (50 diffuse counts or more) in all 5 fields, as long as the cluster has a (0.5 – 2 keV) luminosity of 10^{44} against a typical *Chandra* background. Though the best cluster XLFs are only applicable out to $z \sim 0.8$, this is at least a magnitude ($\sim 3\times$) below L_X^* (Mullis et al. 2004). High L_X ($> 10^{45}$) clusters at higher redshifts are ardently sought, because this is where evolution and cosmological constraints are strongest.

We note that substantial scientific progress is assured even without the proposed Joint *Chandra* or NOAO components. However, the scientific returns are significantly amplified by their inclusion.

⁴All our quasars are at $|b| > 30^\circ$ with low Galactic N_H .

⁵ $\log f_X/f_r = \log f_X(0.5-2\text{keV}) + 5.569 + r'/2.5$

2.2 Technical Plan: NOAO Kitt Peak 4meter

We propose to obtain deep i' , and z' -band imaging of our *Spitzer* sample binary quasars using KPNO 4m + MOSAIC. These data, in combination with IRAC imaging, will allow us to search for possible galaxy density enhancements associated with binary quasars. The MOSAIC+IRAC imaging will enable us to measure photometric redshifts for detected galaxies and resolve early-type cluster red-sequences. Measuring cluster photometric redshifts for our target redshift range ($0.5 \lesssim z \lesssim 3.0$) drives the choice of filters and exposure times. Since the 4000 Å break is redshifted out to 8000 Å by $z = 1$, we require i' and z' imaging to obtain reliable redshifts out to $z \sim 1.4$. For $z > 1.4$ the IRAC 3.6 and 8.0 μm observations will enable us to probe L^* elliptical galaxies to $z < 3$. The (3.6 – 8.0) vs. ($i' - z'$) color-color diagram (see Figure 1b) demonstrates that our chosen filters break the color degeneracy and permit us to measure photo- z s for the required redshift range. The evolution of L^* in the i' , z' , 3.6 μm , and 8.0 μm passbands is calculated using a Bruzual & Charlot (2003) $z_f = 3$ burst model with passive evolution. We select our imaging depths in all filters to probe to at least L^* at the redshift of each target binary quasar.

Good photo- z s demand S/N=5 or better. If we assumed 1'' seeing in bright time, to sample m^* in the $0.5 \lesssim z \lesssim 3$ redshift range we require maximum 90 minute integrations in the i' -band, and 160 min in the z' -band. These exposure times permit us to reach m^* in both filters for our $z > 1.5$ sample and to m^*+3 mag for $z \sim 0.5$. The low-redshift observations will provide us with well-sampled luminosity functions in which to compare our high- z counterparts. We seek to minimize readout overheads, but in these high sky brightness filters, we should not exceed ~ 18 min per exposure. Via multiple dithered exposures, we will avoid saturation effects, maintain a reasonable dynamic range, and also be able to correct for cosmic rays and chip defects.

Photometric calibration for these bands will be bootstrapped from the SDSS, so there is no need to obtain photometric standards. To image our 14 binary quasars and their environments in two filters, we require a total integration time of 9 hours for i' and 20 hours for the z' -band. Including overhead (primarily the 2.5min read-out per image), we require a total of 33 hours, or 3 nights, of KPNO+MOSAIC observing time during the 2007 April/May bright time.

3 Legacy Data Products Plan

Not applicable.

4 Figures and Tables

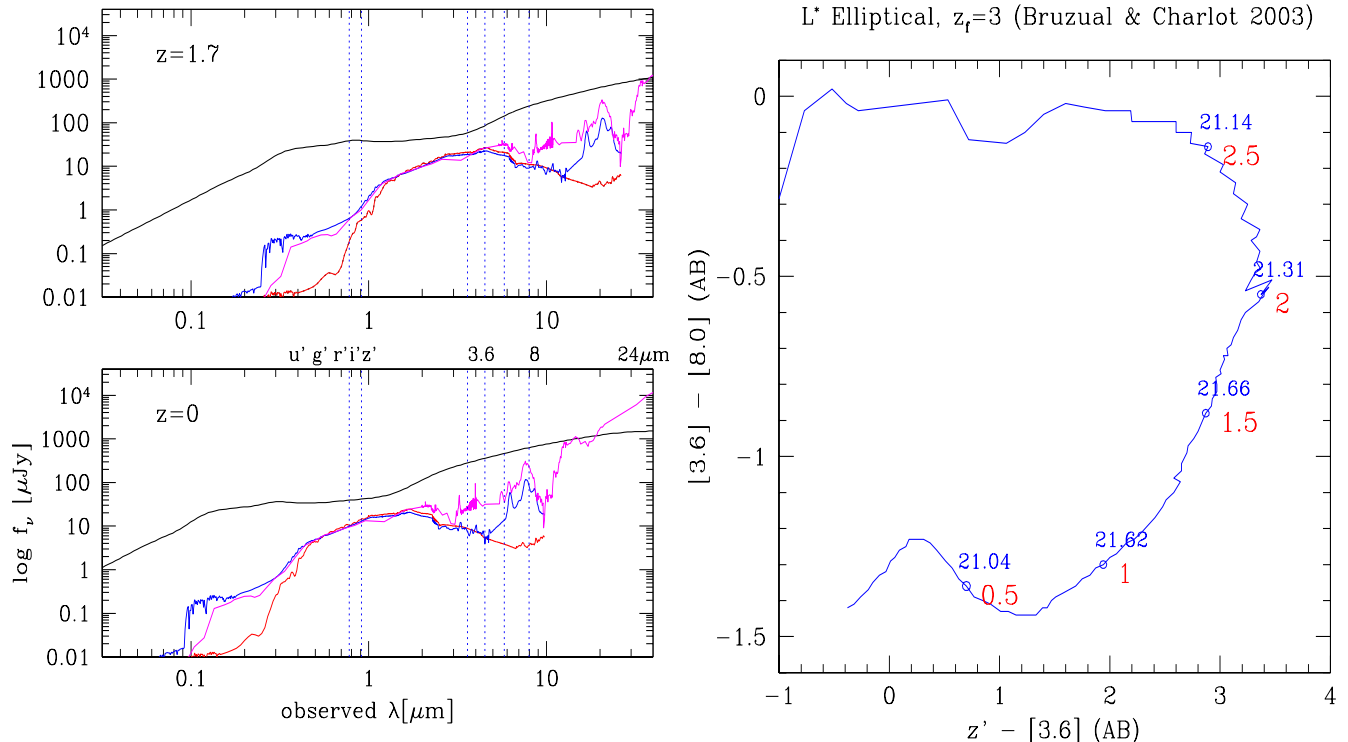


Figure 1: **LEFT:** The *bottom panel* shows the mean SDSS/Spitzer quasar SED from Richards et al. (2006) (black), normalized to our typical SDSS r' magnitudes ~ 20 . Host galaxy SEDs for an elliptical (red), Sbc (blue), or Arp 220 (magenta) are also shown, scaled assuming $L_{Bol}/L_{Edd} = 1$; hosts are even brighter for lower efficiency AGN (§ 1.4). At $z=0$, an Arp220 SED exceeds the quasar SED beginning near $24\mu\text{m}$. Luminous $z=0$ quasars/ULIRGs are already the subject of intense *Spitzer* efforts (e.g., Veilleux, pid 3187), especially those few that have binary nuclei. The *top panel* shows the SEDs at our median sample redshift $z=1.7$. Our 6 proposed IRAC + optical bands are marked by vertical dashed lines. The restframe $1.6\mu\text{m}$ excess falls directly into the IRAC bandpass, optimizing photometric decomposition of the host contributions. **RIGHT:** Expected color track for an L^* elliptical galaxy with a formation redshift of $z=3$ from Bruzual & Charlot (2003). Redshifts are labeled in red along with predicted [8.0] AB mags in blue. The colors we plot here provide high leverage for photometric redshifts and/or red sequence cluster detection. An $8.0\mu\text{m}$ limit of 22mag (AB) is sufficient to characterize a cluster red sequence to $z = 2.5$.

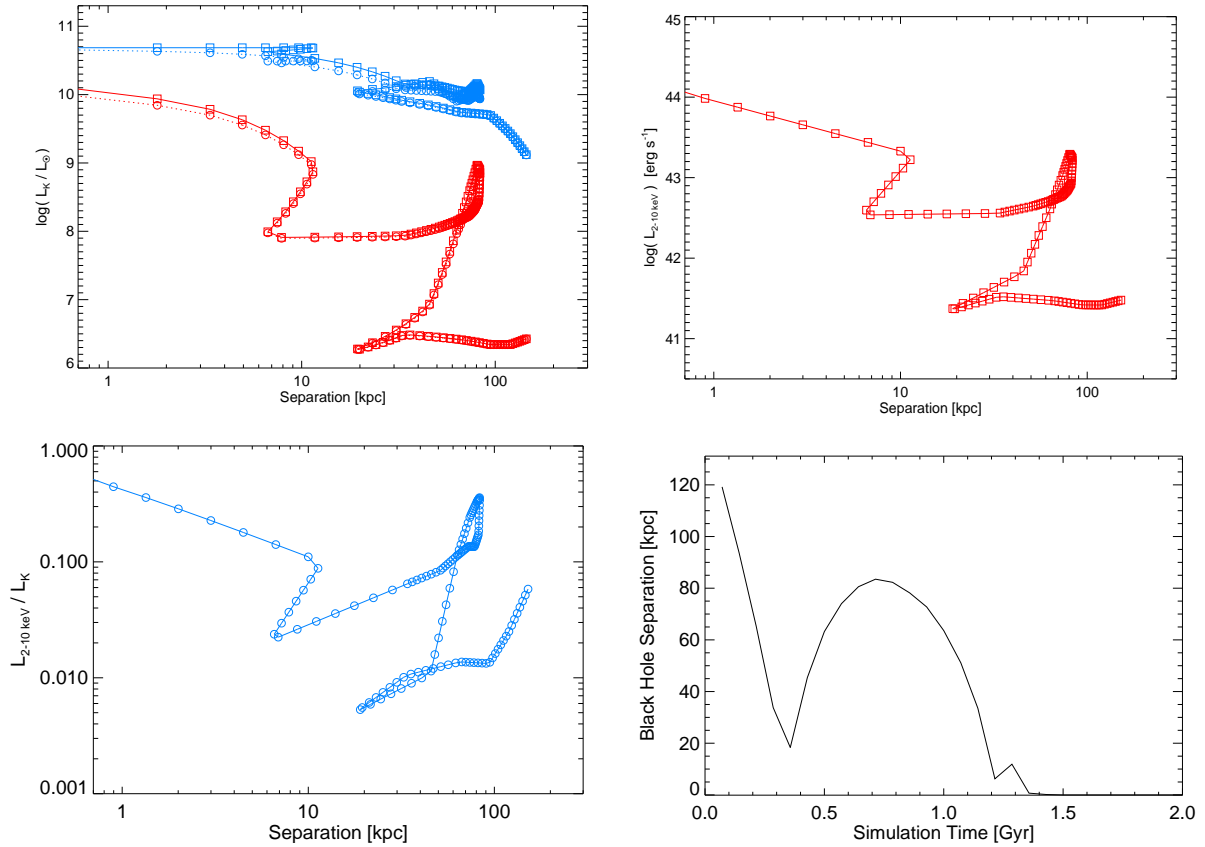


Figure 2: Luminosity trends vs. separation of mergers from our simulations. *Top Left:* Restframe K -band luminosity of host (top curve) and AGN (bottom curve). *Top Right:* X-ray (2-10 keV) luminosity. *Bottom Left:* L_X/L_K . *Bottom Right:* Separation vs. time. All curves are for 2 merging galaxies with initial 40% gas disks, and circular velocity 160 km/sec.

5 References

- Aldcroft, T. L. & Green, P. J. 2003 *ApJ*, 592, 710
Baldwin, J.A. 1977, *ApJ*, 214, 679
Barkhouse, W.A. et al. 2006, *ApJ*, resubmitted (available at public ChaMP website)
Barmby, P. et al. 2006, *ApJ*, in press (astro-ph/0512618)
Bruzual, G., & Charlot, S. 2003, *MNRAS*, 344, 1000
Clowe, D., Gonzalez, A., & Markevitch, M. 2004, *ApJ*, 604, 596
Conselice, C. 2005, *ApJ*, in press (astro-ph/0507146)
Cui, J., et al. 2001, *AJ*, 122, 63
Gladders, M. D., & Yee, H. K. C. 2000, *AJ*, 120, 2148
Granato, G. L., et al. 2004, *ApJ*, 600, 580
Green, P. J., et al. 1995, *ApJ*, 450, 51
——— 2001 *ApJ*, 556, 727
——— 2002, *ApJ*, 571, 721
——— 2004, *MNRAS*, 349, 1261
——— 2005, *ApJ*, 630, 142
Grogin et al 2005, *BAAS*, 207, 6324
Haehnelt, M. G., Davies, M. B., & Rees, M. J. 2006, *MNRAS*, 366, L22
Hennawi, J. F., et al. 2006, *AJ*, 131, 1 (HJ05)
Hopkins, P. F., et al. 2005a, *ApJ*, 630, 705
Kochanek, C. S., Falco, E., Munoz, J. A. 1999, *ApJ*, 510, 590
Khochfar, S., & Burkert, A. 2001, *ApJ*, 561, 517
Komossa, S. et al. 2003, *ApJL*, 582, L15
Lonsdale, C. J., et al. 2003, *PASP*, 115, 897
Lacy, M., et al. 2005, *ApJS*, 161, 41
Merritt, D., & Milosavljević, M. 2005, *Living Reviews in Relativity*, 8, 8
Mortlock, D. J., Webster, R. L.; Francis, P. J. 1999, *MNRAS*, 309, 836
Mullis, C. R. et al. 2004, *ApJ*, 607, 175
Postman, M. 2002, in *ASP Conf. Proc.* 268, *Tracing Cosmic Evolution with Galaxy Clusters*, ed. S. Borgani, M. Mezzetti, & R. Valdarnini (San Francisco: ASP), 3
Russell, D. M., Ellison, S. L., & Benn, C. R. 2006, *MNRAS*, in press (astro-ph/0512210)
Serber, W., Bahcall, N., Menard, B., & Richards, G. 2006, *ApJ*, in press (astro-ph/0601522)
Silverman, J. D., et al. 2005, *ApJ*, 624, 630
Stanford, S. A., et al. 2005, *ApJL*, 634, L129
Strateva, I. V., et al. *AJ*, 130, 387
Teng, S. H., et al. 2005, *ApJ*, 633, 664
Wolf, C., et al. 2003, *A&Ap*, 408, 499
Vanden Berk et al. 2006, *AJ*, 131, 84
Vestergaard, M. & Peterson, B. 2006, *ApJ*, in press (astro-ph/0601303)
Warner, C., Hamann, F., & Dietrich, M. 2004, *ApJ*, 608, 136
Weinstein, M. A., et al. 2004, *ApJS*, 155, 243
White, S. et al 1983, *MNRAS*, 203, 701
Wyithe, J. S. B., & Loeb, A. 2002, *ApJ*, 581, 886
——— 2005, *ApJ*, 634, 910
Zezas, A., Ward, M. J., & Murray, S. S. 2003, *ApJL*, 594, L31

6 Brief Resume/Bibliography

P.I.: Paul J. Green

- Astrophysicist, Chandra Director's Office, Smithsonian Astrophysical Observatory, 2003 –
- NASA Long Term Space Astrophysics Awardee, 1998-2003
- Astrophysicist, Chandra Mission Planning, Smithsonian Astrophysical Observatory, 1996 – 2003
- Hubble Postdoctoral Fellow, Harvard-Smithsonian Center for Astrophysics, 1993 – 1995

SUMMARY CVs

Aldcroft is a Flight Director on the *Chandra* operations team, and an expert on *Chandra* data reduction, specializing in quasars, spectral energy distributions, and combined spatial/spectral analysis.

Barkhouse is a postdoc at U.Illinois, working on deep optical imaging and cluster detection for the Dark Energy Survey. Having led image reduction for the ChaMP survey, Wayne is an expert with deep MOSAIC imaging and data analysis, with scientific emphasis on multiwavelength cluster surveys.

Barmby is part of the IRAC instrument team. Pauline has analyzed data from IRAC GTO program, particularly the Extended Groth Strip, including a study of the infrared properties of X-ray sources in the EGS, and is also studying the properties of Lyman-break galaxies at high-redshift.

Hopkins is a graduate student at Harvard, working with Lars Hernquist on a unified, merger-driven model for the origin of starbursts, quasars, the cosmic X-Ray background, supermassive black holes and galaxy spheroids.

SELECTED RELEVANT PUBLICATIONS of PI and co-Is

- P. Barmby et al. 2006, ApJ, in press (astro-ph/0512618) *Mid-Infrared Properties of X-ray sources in the Extended Groth Strip*
- W. A. Barkhouse, P. J. Green, et al. 2006, ApJ, submitted, *ChaMP Serendipitous Galaxy Cluster Survey*
- P. J. Green, L. Infante, S. Lopez, T. L. Aldcroft, & J. N. Winn 2005, ApJ, 630, 142, *Discovery of a Galaxy Cluster in the Foreground of the Wide-Separation Quasar Pair UM425*
- P. J. Green, T. L. Aldcroft, W. R. Brown and O. Kuhn, 2004, MNRAS, 349, 1261, *HS1216+5032; A Physical Quasar Pair with one Radio-Loud Broad Absorption line Quasar*
- P. J. Green & the ChaMP Collaboration 2004, ApJS, 150, 43, *The Chandra Multiwavelength Project: Optical Followup of Serendipitous Chandra Sources*
- P. Barmby et al. 2004, ApJS 154, 97 *Deep Mid-IR Observations of Lyman-Break Galaxies*
- T. L. Aldcroft & **P. J. Green** 2003 ApJ, 592, 710, *Lens or Binary? Chandra Observations of the Broad Absorption Line Quasar Pair UM425*
- P. J. Green et al. 2002, ApJ, 571, 721, *Chandra Observations of the QSO Pair Q2345+007: Binary Quasar or Massive Dark Lens?*
- P. J. Green, T. L. Aldcroft, S. Mathur, B. J. Wilkes & M. Elvis 2001, ApJ, 558, 109, *A Chandra Survey of Broad Absorption Line Quasars*

7 Observation Summary Table

| Target Field | Position (J2000) | Flux Density | AOT/ Bands | Int./ Pixel (secs) | AOR Duration (secs) | # of AORS |
|-----------------|------------------------|--------------|---------------|--------------------------|---------------------------|--------------|
| SDSSJ0856+5111A | 08:56:25.63+51:11:37.4 | 6uJy | IRAC all | 6700 | 15168 | 1 |

This is an example of one of the 14 final AORs that we are actually submitting. All are similar: the need to achieve adequate depths for Elliptical galaxies in a possible cluster environment automatically achieves the S/N we require for the quasar SEDs, and does not vary much over our redshift range. There are 59 hrs total in IRAC AORs.

A summary of the properties of the full sample is shown at the end of the Scientific Justification section.

8 Status of Existing Observing Programs

P.I. Paul Green is not PI on any other *Spitzer* program.

Co-I P. Barmby is the TC for Fazio GTO program 217 (“Mass Loss in Globular Clusters”). Data for this program have been received and processed; detailed analysis and publication are pending a better understanding of IRAC crowded-field PSF-fitting photometry. Barmby is also the PI of GO-1 program 3126 (“A Complete IRAC Map of M31”): data for this program have been received and mosaiced. A portion of the data have been used in one submitted publication (Marleau et al. 2006), with additional publications in preparation.

9 Proprietary Period Modification

We feel this binary quasar sample is key to testing an important paradigm, one that seeks to unify structure formation with galaxy and AGN evolution. Since these space observatories have limited lifetimes, to stimulate rapid progress we therefore *waive proprietary rights to these data once the approved sample has been observed*.

As co-Chair of the SOC for “Making the Most of the Great Observatories” workshop in Pasadena, May 2006, the PI wishes to encourage the trend of early dissemination of important multiwavelength datasets.

10 Justification of Duplicate Observations

There are no duplicate observations proposed herein.

11 Justification of Targets of Opportunity

There are no ToO observations.

12 Justification of Scheduling Constraints

Most of our targets are at high ecliptic latitude and have low backgrounds (< 7 MJy/sr) at $8\ \mu\text{m}$. For a few that had "medium" backgrounds (up to 10 MJy/src), we have imposed some loose (months-long) time window constraints that bring all targets into the low background regime.

13 Data Analysis Funding Distribution

Example: PI – P. Green (70%), CoI – P. Barmby (30%)

14 Financial Contact Information

Mr. William Ford
Contracting Officer
Mail Stop 23
Smithsonian Astrophysical Observatory
60 Garden Street
Cambridge, MA 02138
617-495-7317
wford@cfa.harvard.edu